Sensors and Materials, Vol. 35, No. 2 (2023) 499–506
MYU Tokyo

S & M 3187

Scintillation Light Yields of Tb-doped SiO_2 Glasses

Noriaki Kawaguchi,[1*] Kenichi Watanabe,[2] Daiki Shiratori,[1]
Takumi Kato,[1] Daisuke Nakauchi,[1] and Takayuki Yanagida[1]

[1]Nara Institute of Science and Technology, 8916-5 Takayama, Ikoma, Nara 630-0192, Japan
[2]Department of Applied Quantum Physics and Nuclear Engineering, Faculty of Engineering, Kyushu University, 744 Motooka, Nishi, Fukuoka 819-0395, Japan

(Received October 12, 2022; accepted January 5, 2023)

Keywords: scintillator, light yield, Tb^{3+} ions, glass

We investigated the scintillation light yields of Tb-doped SiO_2 glasses. We prepared 0.05, 0.1, and 0.5% Tb-doped SiO_2 glasses by melting and solidifying sintered ceramic rods using an oxygen burner. The obtained samples showed no crystalline phases in X-ray diffraction measurements. Pulse height spectra of the Tb-doped SiO_2 samples were measured under γ-ray excitation using a measurement system for slow decay pulses. The number of channels at the Compton edge of the 0.5% Tb-doped sample was the highest and was approximately 50% of that of a commercial lithium glass scintillator (GS20). By considering the light yield of GS20 and the wavelength dependence of the quantum efficiency of the photomultiplier tube, the light yield of the 0.5% Tb-doped SiO_2 sample was estimated as 3800 photons/MeV.

1. Introduction

Scintillators are widely used in radiation detectors for industrial, medical, and scientific applications. Since the properties of scintillators have a significant impact on the performance of radiation detectors, there have been many theoretical and experimental studies on them over the past couple of decades.[1–5] They are still continuing to be studied, and various scintillators such as organic,[6] organic–inorganic hybrid,[7–9] and inorganic materials including fluorides,[10] chlorides,[11–13] bromides,[14,15] iodides,[16] and oxides[17–28] have been investigated over the last few years. In particular, oxide scintillators have attracted considerable attention owing to their excellent chemical stability. They are further classified into single crystals, ceramics, and glasses. However, relatively few oxide glass scintillators are commercially available. As oxide glasses generally have high stability and formability, we believe that further studies of oxide glasses are worthwhile.

Ce-doped lithium silicate glasses are well-known commercial glass scintillators used for thermal neutron detection. These glasses were developed several decades ago;[29] however, their light yields are still the highest among the commercial glass scintillators to the best of our knowledge. The light yields of Ce-doped lithium silicate glass (GS20) under γ-ray and thermal neutron excitation are approximately 4000 photons/MeV and 6000 photons/neutron,

*Corresponding author: e-mail: n-kawaguchi@ms.naist.jp
https://doi.org/10.18494/SAM4136

ISSN 0914-4935
https://myukk.org/

respectively.[2] Hence, glass scintillators have relatively lower light yields than single-crystal scintillators such as NaI:Tl and Lu_2SiO_5:Ce. Birks reviewed early studies on oxide glass scintillators and their low light yields, and he suggested that the efficiency of energy transfer from the host material to the luminescent center is lower in a glass than in a single crystal owing to the absence of any long-range order in the former and the ordered crystal lattice in the latter.[30] However, only Ce-doped glasses with short decay times were intensively evaluated in early studies, and the scintillation properties of glasses with other dopants are still unclear. In particular, the scintillation light yields of glasses with ms-range decay times have not been sufficiently studied, because it is generally difficult to evaluate samples with long decay times using the pulse counting method owing to a lack of commercially available analog modules with a ms-range time constant. On the other hand, Watanabe and our group estimated the light yield of Tb-doped $Sr_2Gd_8(SiO_4)_6O_2$ single crystal as 23000 photons/MeV using a setup for ms ranges.[31] We expect that glasses with ms-range decay times can be measured using a similar method.

In this study, we investigated the scintillation light yields of Tb-doped SiO_2 glasses, which are also called quartz or silica glasses and are among the most well-known glasses. Since SiO_2 glasses have a low effective atomic number, they cannot be regarded as practical scintillators for γ-ray detection. However, they have attractive properties for fundamental studies. The luminescence properties of glasses doped with rare-earth ions have already been studied, including Tb-doped SiO_2 glasses.[32] In addition, the scintillation light yields of SiO_2 glasses doped with Pr^{3+},[33] Eu^{2+},[34] or Sn^{2+}[35] ions, whose decay times are in the ns-to-μs range, have been investigated using the pulse counting method. Since the scintillation light yields of SiO_2 glasses with ms-range decay times have not been intensively studied, they are of interest. In this study, Tb ions were selected as the dopant because we have already succeeded in measuring the light yield of Tb-doped samples.[31]

2. Materials and Methods

We obtained Tb-doped SiO_2 glasses by burner melting.[35] First, mixed powders of Tb_4O_7 (99.99%) and SiO_2 (99.99%) were pressed and formed into rod shapes by hydrostatic pressure. The ratio of Tb ions to Si ions was adjusted to 0.05, 0.1, and 0.5 mol% in the mixed powders. They were heated at 1100 °C for 8 h in air to obtain sintered ceramic rods of Tb-doped SiO_2. One end of each ceramic rod was melted using an oxygen burner (KSA-18; Koshin Rikagaku Seisakusho, Tokyo, Japan) and solidified for a short time. The melted and solidified parts of the rods were cut to approximately 5-mm-diameter discs and their surfaces were polished. X-ray diffraction (XRD) patterns were measured using an X-ray diffractometer with a Cu-Kα X-ray source (MiniFlex600; Rigaku, Akishima, Japan) to determine whether the samples included crystalline phases.

X-ray-induced scintillation spectra were measured using our customized measurement system consisting of an X-ray generator, an optical fiber, and a spectrometer. The samples were irradiated with X-rays using an X-ray generator (XRB80P&N200X4550; Spellman High Voltage Electronics, Hauppauge, New York, United States). Emissions from the samples were transmitted

into a monochromator (Shamrock 163; Andor Technology, Belfast, Northern Ireland) and a CCD-based spectrometer (DU920-BU2NC; Andor Technology) using the optical fiber. The X-ray generator was operated with a tube voltage of 40 kV and a tube current of 1.2 mA. The X-ray-induced scintillation spectrum of a commercial Ce-doped lithium silicate glass (GS20; Scintacor, Cambridge, United Kingdom) was also measured as reference.

Pulse height spectra of the samples and GS20 under γ-ray excitation were measured using a ^{137}Cs sealed source and our customized measurement system to investigate scintillation light yields. This system has a similar concept to that in a previous study.[31] The samples and GS20 were optically coupled with a photomultiplier tube (PMT; R7600U-200; Hamamatsu Photonics) using silicone rubber. Pulse signals from the PMT were analyzed using a preamplifier customized for ms-range pulses (AMP-BNC-03KW; ANSeeN, Hamamatsu, Japan), an analog-to-digital converter (Model 1819-19 2ch ADC; CLEAR-PULSE, Tokyo, Japan), and a personal computer for data acquisition. Each pulse signal was integrated, then the integrated pulse areas and pulse counts were plotted on the horizontal and vertical axes, respectively.

The emission wavelength dependences of the photoluminescence (PL) quantum yields (QYs) of the samples and GS20 were measured using a PL spectrometer (Quantaurus-QY; Hamamatsu Photonics, Hamamatsu, Japan) with 10 nm steps to compensate for effects of the spectral sensitivity of the PMT used in the measurements of the pulse height spectra. PL QYs were measured by integration with 10 nm steps of the emission wavelength under 250 nm excitation, which was the shortest excitation wavelength for this spectrometer. Total QYs were also measured in the excitation wavelength range from 250 to 400 nm.

3. Results and Discussion

Figure 1 shows the appearances of the partially melted and solidified ceramic rods of 0.05, 0.1, and 0.5% Tb-doped SiO_2 under room light and 254 nm UV light and their cut and polished pieces under room light. The melted and solidified parts of the 0.05 and 0.1% Tb-doped SiO_2 ceramic rods were transparent, while that of the 0.5% Tb-doped ceramic rod seemed translucent. The melted and solidified parts showed green emissions under 254 nm UV excitation. Their appearances suggested that the melted and solidified parts of the 0.05 and 0.1% Tb-doped SiO_2 ceramic rods were glasses because melted and solidified transparent inorganic materials are mostly glasses or single crystals, and single crystals are generally obtained only by gradual solidification. The cut and polished disk of the translucent part of the 0.5% Tb-doped ceramic rod seemed almost transparent, whereas the center part of the disk seemed slightly opaque. Assuming that glasses were obtained, we considered that 0.5% is the upper limit of the dopant concentration of Tb-doped SiO_2 glasses prepared by this method. Only low-concentration Tb-doped SiO_2 glasses were also obtained by spark plasma sintering in a previous study.[32] The difficulty in obtaining higher-concentration Tb-doped glasses might be due to the increase in melting temperature upon Tb doping.[36] We used the obtained disks as the samples for this study.

Figure 2 shows the XRD patterns of the Tb-doped SiO_2 samples. No XRD peaks were observed in all the XRD patterns. Even the slightly opaque 0.5% Tb-doped SiO_2 sample showed

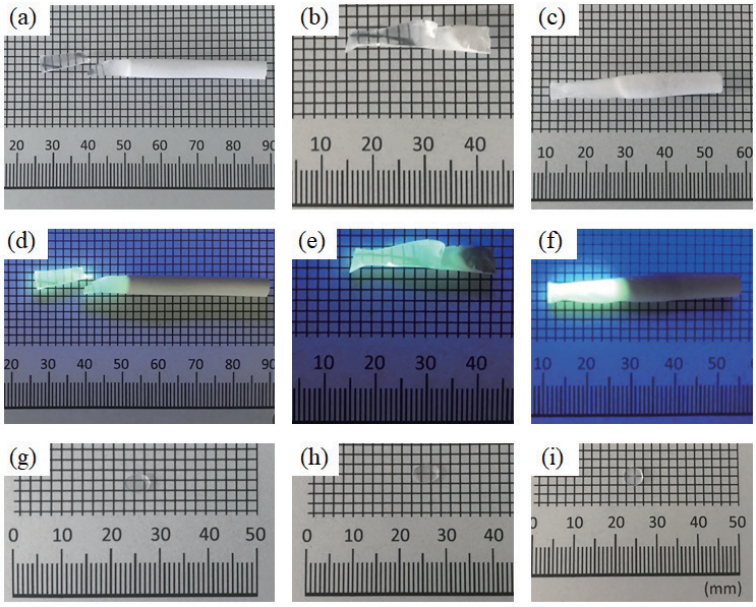

Fig. 1. (Color online) Partially melted and solidified ceramic rods of (a) 0.05, (b) 0.1, and (c) 0.5% Tb-doped SiO_2 under room light; those of (d) 0.05, (e) 0.1, and (f) 0.5% Tb-doped SiO_2 under 254 nm UV light; cut and polished (g) 0.05, (h) 0.1, and (i) 0.5% Tb-doped SiO_2 pieces under room light.

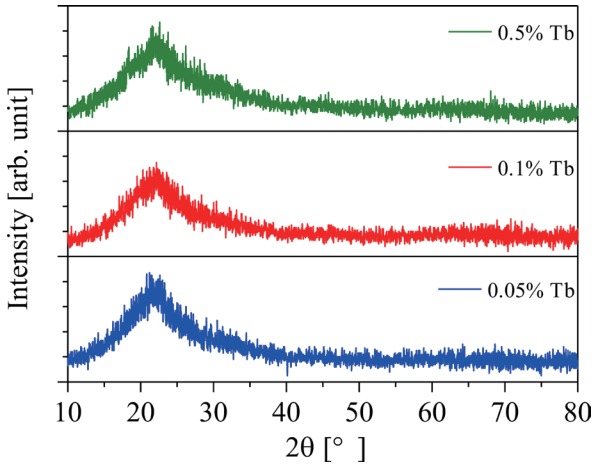

Fig. 2. (Color online) XRD patterns of the Tb-doped SiO_2 samples.

no XRD peaks using this measurement method. Because all the samples seemed to show no or few crystalline components, they were considered to have mainly glass components. Hereafter, the samples are thus described as glasses.

Figure 3 shows X-ray-induced emission spectra of the Tb-doped SiO_2 glasses and GS20. The thicknesses of the 0.05, 0.1, and 0.5% Tb-doped SiO_2 glass samples were 0.54, 0.82, and 0.74 mm, respectively, similar to that of GS20 (1.05 mm). Although this measurement method has

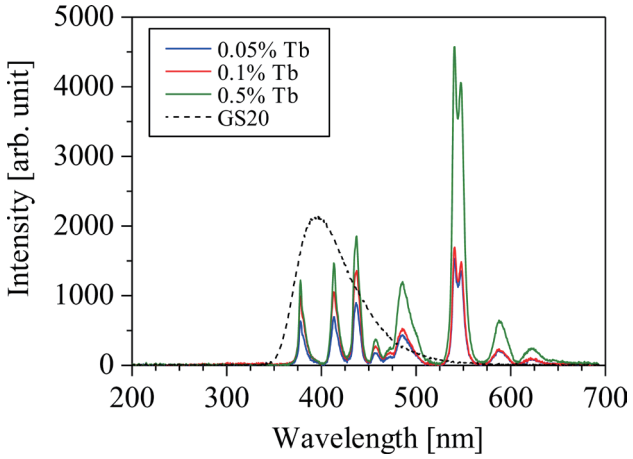

Fig. 3. (Color online) X-ray-induced emission spectra of the Tb-doped SiO_2 glasses and GS20.

low quantitativity, the scintillation intensities of the Tb-doped SiO_2 glasses and GS20 were considered to be similar. The emission peaks of the Tb-doped SiO_2 glass samples can be ascribed to 4f-4f transitions of Tb^{3+} ions, as well as those of the Tb-doped SiO_2 glasses obtained by spark plasma sintering in the previous study.[32]

Figure 4 shows the pulse height spectra of the Tb-doped SiO_2 glasses and GS20 under γ-ray excitation from a ^{137}Cs sealed source. All the samples showed Compton edges separated from the noise level, whereas no photoelectric absorption peaks were observed owing to the low effective atomic number. The 0.5% Tb-doped SiO_2 glass showed the Compton edge with the highest number of channels among the Tb-doped SiO_2 glass samples. The number of channels at the Compton edge of the 0.5% Tb-doped SiO_2 glass (around 100 channels) was approximately 50% of that of GS20 (around 200 channels). This comparison is affected by the wavelength dependence of the quantum efficiency of the PMT.

To investigate the changes in the emission spectra, we measured PL emission spectra and QYs of the samples and GS20. Excitation wavelengths were set from 250 to 400 nm because 250 nm was the shortest excitation wavelength of our measurement device and 400 nm was a sufficiently long wavelength for the emission wavelengths of the samples and GS20 (suitable excitation wavelengths are generally lower than the emission wavelengths). The PL QYs of the samples and GS20 depended on the excitation wavelength. When we integrated the spectra over the whole emission wavelength range, we obtained maximum PL QYs of the 0.05, 0.1, and 0.5% Tb-doped SiO_2 glass samples of 24.4 33.0 and 22.1%, respectively. These maximum PL QYs were obtained under 250 nm excitation. Although the PL intensity of the 0.5% Tb-doped sample was higher than that of the 0.1% Tb-doped sample, the PL QY of the 0.5% Tb-doped sample was lower than that of the 0.1% Tb-doped sample. This was due to the optical absorbance of the 0.5% Tb-doped sample (34.4%) being higher than that of the 0.1% Tb-doped sample (13.6%) for excitation light. Since the PL QY is calculated as the ratio of the number of emitted photons to the number of absorbed photons, it can be decreased by adsorbates in samples with no emissions. The 0.5% Tb-doped sample had a slightly opaque part, and this component may have acted as an

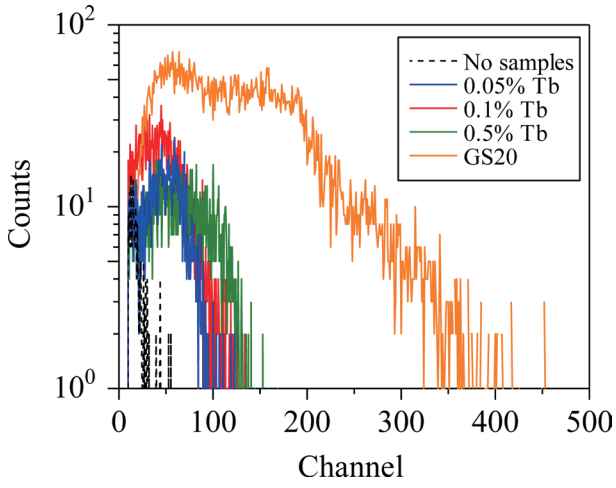

Fig. 4. (Color online) Pulse height spectra of the Tb-doped SiO_2 glasses and GS20 under γ-ray excitation from a ^{137}Cs sealed source.

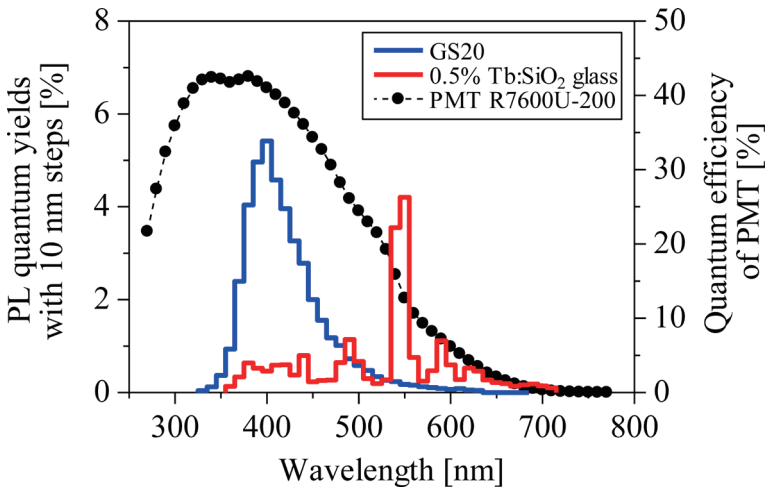

Fig. 5. (Color online) Wavelength dependence of PL QY of the 0.5% Tb-doped SiO2 glass and GS20 integrated with 10 nm steps under 250 nm excitation and the wavelength dependence of the quantum efficiency of PMT R7600U-200.

adsorbate with no emissions. The maximum PL QY of GS20 was 80.0% under 340 nm excitation, while the PL QY under 250 nm excitation was 42.1%. The tail of the PL emission spectrum of GS20 overlapped with the excitation light spectrum under 340 nm excitation. When we selected 250 nm as the excitation wavelength, the spectra of the excitation light were sufficiently separated from the emission spectra of the 0.5% Tb-doped sample and GS20. In addition, the PL emission spectra of GS20 at excitation wavelengths from 250 to 340 nm seemed to have almost the same shape. Therefore, we used the emission wavelength dependence of the PL QY under 250 nm excitation to evaluate the PL spectral shape. Figure 5 shows the wavelength dependence of the PL QY of the 0.5% Tb-doped SiO_2 glass and GS20 integrated with 10 nm steps under 250

nm excitation and the wavelength dependence of the quantum efficiency of PMT R7600U-200 obtained from the spec sheet of this PMT. The average quantum efficiency of the PMT relative to those of the 0.5% Tb-doped sample and GS20 was calculated from the product of the ratio of the PL QY of each integrated wavelength region to the total PL QY integrated in the whole emission wavelength range and the quantum efficiency of the PMT corresponding to each wavelength range. The average quantum efficiencies of the PMT for the 0.5% Tb-doped SiO_2 glass and GS20 were 19.32 and 36.84%, respectively. If the light yield of GS20 is 4000 photons/MeV,[2] then that of the 0.5% Tb-doped SiO_2 glass can be estimated to be 3800 photons/MeV by a comparison of the numbers of channels at the Compton edges in Fig. 4. The estimated value is consistent with those of glasses with relatively low light yields.

4. Conclusions

We prepared 0.05, 0.1, and 0.5% Tb-doped SiO_2 glass samples and investigated their light yields. We confirmed that the samples showed no crystalline phases in XRD measurements and that they showed emissions due to 4f-4f transitions of Tb^{3+} ions in X-ray-induced scintillation spectra. The pulse height spectra of the samples were measured and compared with that of GS20. The 0.5% Tb-doped SiO_2 sample showed the highest light yield, and its value was estimated to be 3800 photons/MeV by compensation using the quantum efficiency of PMT and the wavelength dependence of the PL QYs of the sample and GS20. The light yield of the Tb-doped SiO_2 glass was considered to be relatively low and similar to that of general glass scintillators.

Acknowledgments

This work was supported by Grants-in-Aid for Scientific Research A (22H00309), Scientific Research B (21H03733, 21H03736, 22H02939, and 22H03872), and Exploratory Research (22K18997) from Japan Society for the Promotion of Science. Part of this research is based on the Cooperative Research Project of Research Center for Biomedical Engineering.

References

1 G. F. Knoll: Radiation Detection and Measurement (Wiley, New York, 2010) 4th ed.
2 C. W. E. van Eijk: Nucl. Instrum. Methods Phys. Res., Sect. A **460** (2001) 1.
3 S. E. Derenzo, M. J. Weber, E. Bourret-Courchesne, and M. K. Klintenberg: Nucl. Instrum. Methods Phys. Res., Sect. A **505** (2003) 111.
4 C. W. E. van Eijk, A. Bessière, and P. Dorenbos: Nucl. Instrum. Methods Phys. Res., Sect. A **529** (2004) 260.
5 T. Yanagida: Opt. Mater. **35** (2013) 1987.
6 A. Watanabe, A. Magi, M. Koshimizu, A. Sato, Y. Fujimoto, and K. Asai: Sens. Mater. **33** (2021) 2251.
7 M. Koshimizu, N. Kawano, A. Kimura, S. Kurashima, M. Taguchi, Y. Fujimoto, and K. Asai: Sens. Mater. **33** (2021) 2137.
8 K. Okazaki, D. Onoda, D. Nakauchi, N. Kawano, H. Fukushima, T. Kato, N. Kawaguchi, and T. Yanagida: Sens. Mater. **34** (2022) 575.
9 D. Onoda, M. Akatsuka, N. Kawano, T. Kato, D. Nakauchi, N. Kawaguchi, and T. Yanagida: Sens. Mater. **34** (2022) 585.
10 Y. Zheng, H. Xu, X. Xu, L. Xu, S. Wang, and S. Wu: J. Alloys Compd. **910** (2022) 164778.

11 D. Rutstrom, L. Stand, C. Delzer, M. Kapusta, J. Glodo, E. Loef, K. Shah, M. Koschan, C. Melcher, and M. Zhuravleva: Opt. Mater. **133** (2022) 112912.
12 Y. Fujimoto, D. Nakauchi, T. Yanagida, M. Koshimizu, and K. Asai: Sens. Mater. **34** (2022) 629.
13 G. Ito, H. Kimura, D. Shiratori, D. Nakauchi, T. Kato, N. Kawaguchi, and T. Yanagida: Sens. Mater. **34** (2022) 685.
14 J. Xiong, X. Zhang, H. Zhou, Y. Shen, S. Pan, Y. Wu, H. Chen, and J. Pan: J. Cryst. Growth **593** (2022) 126740.
15 H. Kimura, T. Kato, D. Nakauchi, N. Kawaguchi, and T. Yanagida: Sens. Mater. **34** (2022) 691.
16 X. Niu, J. Xiao, B. Lou, Z. Yan, Q. Zhou, T. Lin, C. Ma, and X. Hana: Ceram. Int. **48** (2022) 30788.
17 Y. Fujimoto, D. Nakauchi, T. Yanagida, M. Koshimizu, and K. Asai: Sens. Mater. **33** (2021) 2147.
18 T. Yanagida, Y. Fujimoto, H. Masai, G. Okada, T. Kato, D. Nakauchi, and N. Kawaguchi: Sens. Mater. **33** (2021) 2179.
19 P. Kantuptim, H. Fukushima, H. Kimura, D. Nakauchi, T. Kato, M. Koshimizu, N. Kawaguchi, and T. Yanagida: Sens. Mater. **33** (2021) 2195.
20 D. Nakauchi, T. Kato, N. Kawaguchi, and T. Yanagida: Sens. Mater. **33** (2021) 2203.
21 N. Kawaguchi, H. Masai, M. Akatsuka, D. Nakauchi, T. Kato, and T. Yanagida: Sens. Mater. **33** (2021) 2215.
22 H. Fukushima, M. Akatsuka, H. Kimura, D. Onoda, D. Shiratori, D. Nakauchi, T. Kato, N. Kawaguchi, and T. Yanagida: Sens. Mater. **33** (2021) 2235.
23 M. Akatsuka, H. Kimura, D. Onoda, D. Shiratori, D. Nakauchi, T. Kato, N. Kawaguchi, and T. Yanagida: Sens. Mater. **33** (2021) 2243.
24 T. Yanagida, T. Kato, D. Nakauchi, and N. Kawaguchi: Sens. Mater. **34** (2022) 595.
25 P. Kantuptim, D. Nakauchi, T. Kato, N. Kawaguchi, and T. Yanagida: Sens. Mater. **34** (2022) 603.
26 D. Nakauchi, H. Fukushima, T. Kato, N. Kawaguchi, and T. Yanagida: Sens. Mater. **34** (2022) 611.
27 T. Kunikata, T. Kato, D. Shiratori, D. Nakauchi, N. Kawaguchi, and T. Yanagida: Sens. Mater. **34** (2022) 661.
28 N. Kawaguchi, D. Nakauchi, T. Kato, Y. Futami, and T. Yanagida: Sens. Mater. **34** (2022) 725.
29 A. R. Spowart: Nucl. Instrum. Methods **135** (1976) 441. https://doi.org/10.1016/0029-554X(76)90057-4
30 J. B. Birks: The Theory and Practice of Scintillation Counting (Pergamon Press, London, 1964) Chap. 13.
31 K. Watanabe, T. Yanagida, D. Nakauchi, and N. Kawaguchi: Jpn. J. Appl. Phys. **60** (2021) 106002.
32 K. Ichiba, Y. Takebuchi, H. Kimura, T. Kato, D. Shiratori, D. Nakauchi, N. Kawaguchi, and T. Yanagida: Radiat. Phys. Eng. **202** (2023) 110515.
33 Y. Sun, M. Koshimizu, S. Kishimoto, and K. Asai: J. Sol-Gel. Sci. Technol. **62** (2012) 313. https://doi.org/10.1007/s10971-012-2726-6
34 Y. Fujimoto, T. Yanagida, M. Koshimizu, and K. Asai: Sens. Mater. **27** (2015) 263.
35 D. Shiratori, H. Kimura, D. Nakauchi, T. Kato, N. Kawaguchi, and T. Yanagida: Radiat. Meas. **134** (2020) 106297.
36 N. Wolff and D. Klimm: J. Solid State Chem. **312** (2022) 123269.